where

$$\left.\begin{aligned}
K_1 &= \frac{(m\pi)^3}{12(1-\mu^2)}\left(\frac{t}{L}\right)^2\left(\frac{R}{L}\right) \qquad p = \frac{(m\pi)^2}{12(1-\mu^2)}\left(\frac{t}{L}\right)^2 \\
K_2 &= \frac{(m\pi)^2}{3(1-\mu^2)}\left(\frac{t}{L}\right)\left(\frac{t}{b}\right)\left(\frac{t}{d}\right)\left(\frac{R}{L}\right) \\
K_3 &= \frac{1}{2(1-\mu^2)}\left(\frac{t}{d}\right)^2\left(\frac{t}{b}\right)\cos\psi_0 \\
K_4 &= \frac{(m\pi)^2}{2(1-\mu^2)}\left(\frac{t}{d}\right)^2\left(\frac{t}{b}\right)\left(\frac{R}{L}\right)\sin\psi_0 \qquad K_5 = \cos\psi_0 \\
K_6 &= -\frac{(m\pi)^3}{12(1-\mu^2)}\left(\frac{t}{L}\right)^2\left(\frac{R}{L}\right)\sin\psi_0 \\
K_7 &= \frac{m\pi}{2(1-\mu^2)}\left(\frac{t}{d}\right)^2\left(\frac{t}{b}\right)\left(\frac{R}{L}\right) \\
K_8 &= \frac{1}{(m\pi)(1-\mu^2)}\left(\frac{L}{t}\right)\left(\frac{t}{b}\right)\left(\frac{t}{d}\right)^3\cos\psi_0 \\
K_9 &= \frac{1}{(1-\mu^2)}\left(\frac{t}{d}\right)^3\left(\frac{t}{b}\right)\left(\frac{R}{t}\right)\sin\psi_0
\end{aligned}\right\} \quad \text{(A14)}$$

References

[1] Fung, Y. C. and Sechler, E. E., "Instability of Thin Elastic Shells," *Structural Mechanics, Proceedings of the First Symposium on Naval Structural Mechanics*, Pergamon Press, New York, 1960.

[2] Flügge, W., *Handbook of Engineering Mechanics*, McGraw-Hill, New York, 1962.

[3] Gerard, G. and Becker, H., *Handbook of Structural Stability*, Party III: "Buckling of Curved Plates and Shells," TN 3783, 1957, NACA.

[4] Gerard, G., *Handbook of Structral Stability*, Supplement to Part III, "Buckling of Curved Plates and Shells," TN D-163, 1959, NACA.

[5] Batdorf, S. B., "A Simplified Method of Elastic Stability Analysis for Thin Cylindrical Shells," Rept. 874, 1947, NACA.

[6] Leggett, D. M. A., "The Elastic Stability of a Long and Slightly Bent Rectangular Plate under Uniform Shear," *Proceedings of the Royal Society of London*, Ser. A, Vol. 162, 1937, p. 62.

[7] Chu, K. H. and Krishnamoorthy, G., "Buckling of Open Cylindrical Shells," *Proceedings of ASCE, Journal of the Engineering Mechanics Division*, Vol. 93, No. EM 2, April 1967.

[8] Donnell, L. H., "Stability of Thin Walled Tubes under Torsion," Rept. 479, 1933, NACA.

OCTOBER 1974 AIAA JOURNAL VOL. 12, NO. 10

Flowfield Measurements in an Asymmetric Axial Corner at $M = 12.5$

JAMES R. COOPER* AND WILBUR L. HANKEY JR.†
Aerospace Research Laboratories, Wright-Patterson Air Force Base, Ohio

A detailed study of shock-wave boundary-layer interaction and interference heating of an axial corner typical of vehicle junctions has been made. Extensive impact pressure profiles were obtained in addition to static pressure information and oil flow studies. Measurements revealed two large vortices within the boundary layer responsible for high local heating. A complex inviscid shock pattern dominated by a triple point structure was also determined.

Nomenclature

h = heat-transfer coefficient (Btu/ft^2-sec-°F)
M = Mach number
p = static pressure
p_I = impact pressure
R = flow reattachment location
S = flow separation location
Y = conical y value normalized with respect to x
Z = conical z value normalized with respect to x
ξ = static pressure ratio

Subscripts

c = cross flow component
T = values related to triple point

Presented as Paper 73-676 at the AIAA 6th Fluid and Plasma Dynamics Conference, Palm Springs, Calif., July 16–18, 1973; submitted July 26, 1973; revision received May 16, 1974.

Index categories: Boundary Layers and Convective Heat Transfer—Laminar; Jets, Wakes, and Viscid-Inviscid Flow Interactions; Supersonic and Hypersonic Flow.

* Captain, U.S. Air Force, Hypersonic Research Laboratory.

† Senior Scientist, Hypersonic Research Laboratory. Member AIAA.

Introduction

IN the design of an aerodynamic body subject to hypersonic flow it is important to understand the nature of the flowfield that will develop around the body. One of the most important reasons for understanding the flow is due to its high heating potential, not only in stagnation regions, but near flow interference regions as well. Often in hypersonic flow bow shocks generated by various portions of a configuration will trigger boundary-layer flow separation. The separated flow, after negotiating the adverse pressure gradient presented by the shock, will attach itself to the surface and cause heating rates at reattachment which can sometimes exceed those at the leading edge stagnation regions. Without adequate knowledge of this three-dimensional separation and reattachment phenomena and its associated heating capability, a design may not properly account for the higher heating rates and subsequent structural failure could occur.

One of the more common configurations that cause shock-induced boundary-layer separation is the axial corner, typically occurring on a vehicle at such locations as the wing body, body tail, or inlet junctions. Strong bow shocks are generated by the surfaces of an axial corner. The bow shock generated by one surface impinges on the boundary layer of the second surface

imposing an adverse presure gradient on the flow. As a result of this pressure gradient, multiple separation regions can occur which, in three-dimensional separation, will scavenge off the low-energy flow of the boundary layer. The flow then consists of high-energy air which causes the elevated heating rates experienced in the reattachment region of the surface.

Because of the bow-shock induced-separation characteristics of an axial corner, the corner configuration was selected to generate the hypersonic flowfield studied in this investigation. To enhance the separation features of the axial corner, the boundary layer to be separated was developed on a surface aligned with the flow to insure that the bow shock of the surface would be weak and the boundary layer large. The second surface was inclined so that the flow would be compressed and a strong bow shock generated. Because of these requirements, the axial corner configuration selected was highly asymmetric, consisting of a wedge and a flat plate. Data from the asymmetric axial corner, which is presented here, were acquired for the purpose of satisfying the following basic objectives of this program: 1) determining the flowfield structure in a highly asymmetric axial corner, and 2) associating areas of local elevated heating rates with the accompanying flowfield phenomena.

Model and Apparatus

Model and Facility

As indicated in Fig. 1 the shock interference corner flow model used for this study consists of a flat plate with a 15° wedge located along the right-hand side. The flat plate is 16-in. long and 8-in. wide with a sharp 20°-bevel leading edge. The surface of the plate aft of the leading edge is a removable instrumented steel insert containing static pressure ports in 43 locations. A recessed base plate, to which the insert is secured, provides an access path for the necessary pressure tubing.

A 6-in. high, 16-in. long wedge shock generator is positioned on the flat plate at a 15° angle of incidence using two brackets to hold it in place. The leading edge of the wedge is sharp with a 20° bevel.

The plate and wedge assembly were mounted in the ARL 20-in. Hypersonic Wind Tunnel facility with the plate at 0° angle of attack and the wedge presenting a 15° compression surface to the flow. The 20-in. HWT has an open flow test section with a usable uniform flow core of about 10 in. in diameter. Support of the model is provided through a sting mount arrangement which can retract the model from the flow for tunnel starting.

Throughout the investigation the flow conditions in the 20-in. tunnel were held constant. All data were gathered at a Mach number of 12.5 with a total temperature of 1800°R and a total pressure of 1200 psia. The flow was fully laminar with a free-stream Reynolds number of 0.93 million per ft.

Instrumentation

Data on the flow conditions in the axial corner were gathered in three ways. Static pressure was recorded at 43 locations on the flat plate, an extensive impact pressure survey was conducted, and an oil flow technique was employed to aid in flow visualization.

The static pressure ports on the plate were connected by pressure lines, passing through the sting support, to pressure transducers mounted in the test cabin. Signals from the transducers were fed from the test cabin to an Ambilog data recording system where pressures were recorded at one second intervals throughout each run. Because only 25 transducer channels were available for any given run, two runs were required to record all 43 static pressures for the given running conditions. To insure uniform flow conditions, two ports from the first run were also recorded during the second run and compared to see that the same values were indicated. Before each day of running, all the transducers were calibrated against a known pressure source and again checked against the source after the running was complete. The two-run series was rerun several times to check on the repeatability of the tunnel flow conditions as well as the data acquisition system.

Impact pressure information was acquired through the use of a tunnel-mounted computer-controlled probe system capable of movement along three axes. An extensive survey program was conducted in which the corner flow structure was probed in three different y-z planes. For a given x location, a constant y value was fed to the probe and the z value was stepped in 0.1 in. increments. The probe traveled 12 in. in the -z direction until it contacted the wedge surface then returned to its original location to complete each run. The average time per run was about 90 sec. After each run the y location of the probe was increased 0.1 in. and the procedure repeated. In this way the entire flow structure of the corner was mapped on a matrix of impact pressure points with 0.1 in. spacing. Three y-z planes were mapped, but only the data obtained at the last station, $x = 12.5$ in., were used extensively in this study because of the increased relative fineness of the matrix at that station with respect to the flow structure.

The probe was constructed of 0.093 in. i.d. steel tubing filed to a sharp leading edge. The face of the probe was aligned approximately 7° off the freestream direction toward the wedge surface to keep alignment errors to a minimum. Lag time in the probe system was accounted for by allowing the probe to "rest" at the end of each 0.1 in. movement before the pressure was recorded. This procedure was demonstrated to be adequate by superimposing data taken in opposite directions of probe travel. No displacement of pressure discontinuities was observed indicating that any lag in the probe data system had been accounted for.

To aid in visualizing the flow structure, several oil flow runs were made. After some experimentation, it was found that discrete oil dots provided the most clearly defined surface structure. Flow separation and reattachment lines could be identified from the flow pattern by observing whether the oil flow lines were converging or diverging. Convergence was interpreted as a flow separation region and divergence as a reattachment line.

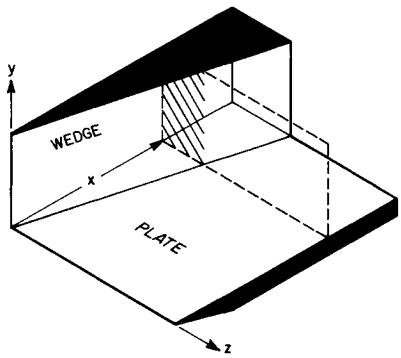

Fig. 1 Corner flow model and coordinate system.

Discussion of the Inviscid Model

To accomplish an objective of this study, reconstruction of the asymmetric axial corner flowfield, it is useful to first consider the entirely inviscid case for the 15° wedge-flat plate corner. For reconstruction purposes it is possible to assume that the flow is conical in nature, which is to say that the flow structure grows in a linear manner with x. This assumption was qualitatively confirmed in the oil flow tests. Figure 2 depicts the ideal inviscid flow structure in an arbitrary y-z plane of the corner configuration. In the freestream, the "cross-flow streamlines" are directed toward the x-axis of the model. Upon encountering the wedge shock, however, the "streamlines" are adjusted such that the flow is in the direction of the wedge-plate intersection line. This line, toward which all the "cross-flow streamlines" finally converge, is termed a vortical singularity. In the immediate

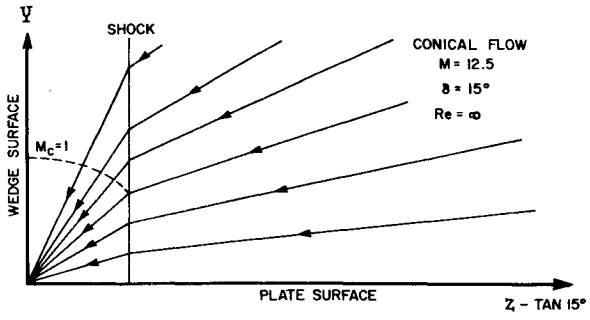

Fig. 2 Ideal inviscid flow.

vicinity of the vortical singularity the cross-flow Mach number, M_c, is subsonic so that there exists in the flow a cross-flow sonic line where $M_c = 1$.

Now, if a viscous displacement effect is allowed on the flat plate so that it appears as a compression surface to the flow, the resulting inviscid structure becomes more realistic. Figure 3 illustrates the new inviscid model which now presents the inviscid flow structure of a highly asymmetric double wedge axial corner in which two bow shocks are now present. Given a nominal compression thickness seen by the freestream flow for the wedge and the plate, a location as well as a strength can be associated with each bow shock in this model. Using the location of the shocks, it is a simple matter to find a set of coordinates in the cross-flow plane which represent the location of the intersection of the bow shocks. For convenience the coordinates are represented as Z_T and Y_T which are the z and y values normalized with respect to the x location of the z-y plane of interest.

In conical flow the location of two intersecting shocks (Z_T, Y_T) is sufficient to completely describe the resulting flowfield around the point of intersection. The intersecting bow shocks in conical flow form a triple point with a third embedded shock and a slip surface which are detailed in Fig. 3. It is this embedded shock which sets up the adverse pressure gradient causing separation. Flow passing through the wedge bow shock will acquire a new value of pressure and cross-flow angle. As a result of the nature of the slip surface in the corner which cannot support a pressure or flow direction mismatch, the values of pressure and flow angle across it must be identically equal. An iteration process is required to simultaneously solve the appropriate relationships for the flow values around the triple point.

By simultaneously solving the shock relationships for a triple point, a Gonar-like[1] solution was found which is represented by the structure of Fig. 3. Examination of the resultant inviscid model shows that the "cross-flow streamlines" again are directed toward the x-axis in the freestream. As the cross flow passes through the wedge and plate bow shocks, the "streamlines" acquire a direction toward two separate singularity points. The flow of the wedge bow shock reaches a vortical singularity in the inviscid model, but the flow of the plate bow shock is turned again by the embedded shock and the "streamlines" are turned to a new vortical singularity deep in the corner. In an inviscid solution of a conical flow problem a vortical singularity indicates the conical ray toward which the cross-flow "streamlines" move. In the present solution the singularity indicates the presence of an inviscid finger deep in the corner flow. In reality the inviscid finger will never reach a vortical singularity due to viscous effects. It is this inviscid finger of high-energy cross flow, with a high value of impact pressure, that will be shown to have a significant effect in the high local heating of the plate.

Information given in earlier corner flow studies[2,3] using symmetric or nearly symmetric corners noted that the bow shocks of the two surfaces did not intersect directly but formed two separate triple points joined by a diagonal shock in the corner. Each triple point generated an embedded shock which extended toward the body surface where it caused the flow to separate. Slip surfaces which extended toward the corner were also generated at the triple points. In the highly asymmetric case modeled above, however, only one triple point is found instead of two. The condition that probably influences this most comes from the previously noted fact that near a vortical singularity the cross flow Mach number is less than one, such that a sonic line ($M_c = 1$) exists in the flow. In the symmetric case, the sonic line in the cross flow behind the wedge shock exists inboard of the bow shock intersection, whereas the shock intersection occurs inboard of the sonic line for the highly asymmetric case. Since imbedded shocks cannot exist in subsonic cross flow, the conditions for a second triple point cannot be met in the asymmetric corner. However, because the cross flow is subsonic, the wedge bow shock is capable of curving near the point of the bow shock interaction, negating the need for a second triple point and allowing the corner flow structure to exist with one triple point. Note that the sonic line, indicated in Fig. 3, is located well outboard of the triple point. From the above discussion the wedge bow shock below the sonic line can be expected to be curved to meet the triple point at the required slope. This conclusion is supported by data discussed in the following section.

Because of the uncertainty of what flow conditions may influence the existence of one or two triple points for a given configuration, a prediction cannot be made as to the type of flow that will exist for configurations and conditions different from those studied in this paper. The present study has not determined just how asymmetric the model must be to produce a single triple point configuration. It is noted that Charwat and Redekopp have found two triple points in a 12.2°, 3.5° corner. This, however, is significantly less asymmetric than the 15.7°, 2.1° corner of this paper, which may account for the difference in the flow configurations. Kutler[4] has shown a two triple point

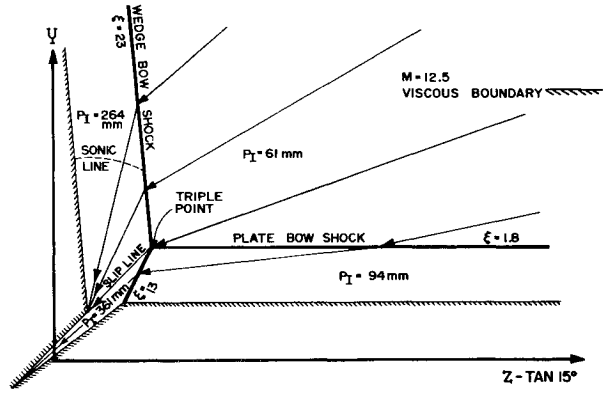

Fig. 3 Inviscid flow with viscous effects.

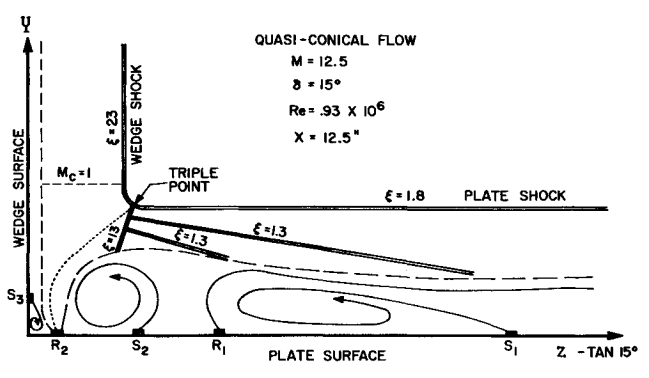

Fig. 4 Salient features of flow structure.

configuration in similar asymmetric corners using a finite-difference numerical approach. The method he has used, however, does not fully account for viscous effects in a strong viscous-inviscid environment. For this reason Kutler's approach may fail to indicate the loss of one of the triple points under certain flow conditions.

Discussion of Test Data

Figure 4 summarizes the salient flow features deduced from the experimental test data of this investigation. The primary inviscid flowfield structure was obtained from the impact

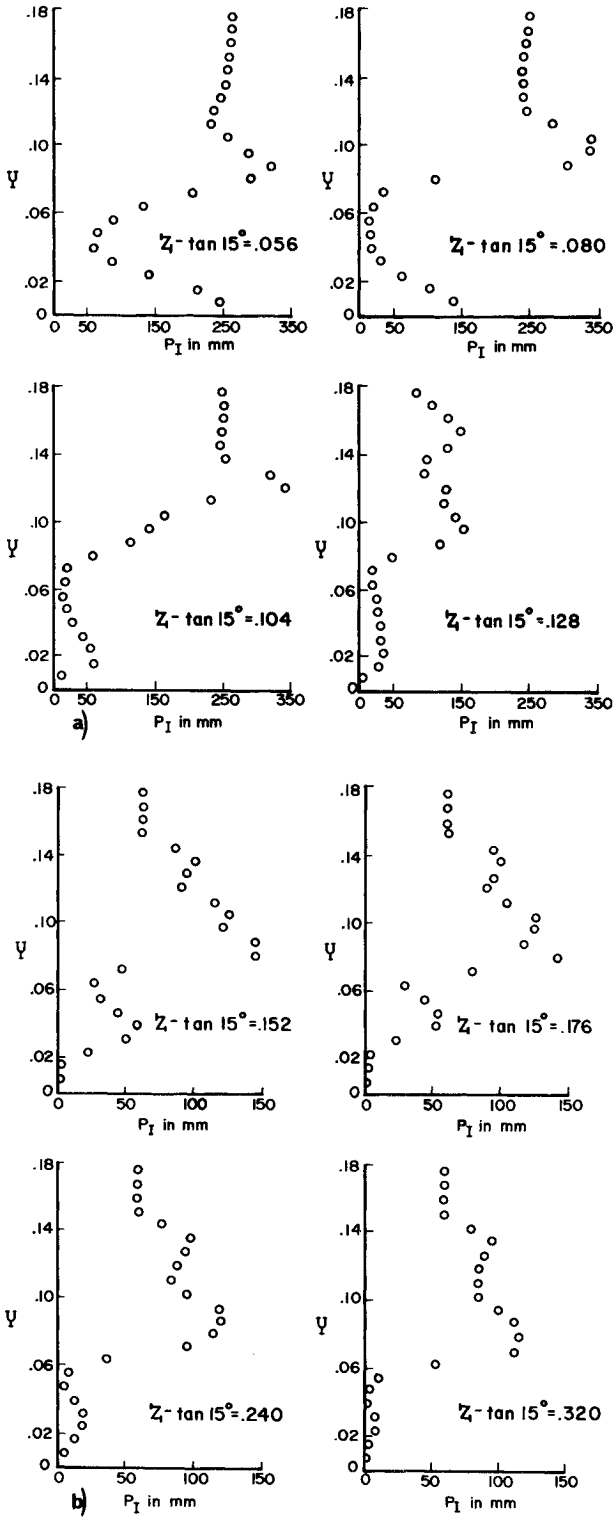

Fig. 5 Impact pressure profiles at various Z values.

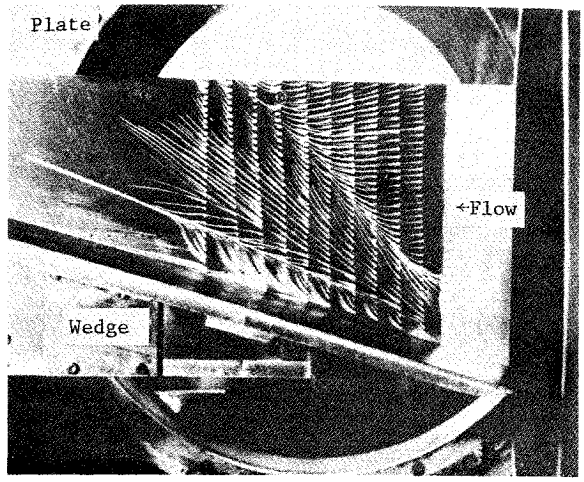

Fig. 6 Oil flow on plate surface.

pressure information and coupled to the viscous structure obtained from the static pressure and oil flow data. Discontinuities in the flowfield were identified by plotting any large discontinuities in impact pressure values in a field of more than 1500 readings taken at $x = 12.5$ in. As an example, for the wedge shock location a line was established separating the impact pressures of the freestream value of 61 mm from those reading about 250 mm behind the shock. Thus the location of a shock with a strength of p_2/p_1 equaling 23 was established. In a similar manner, the entire flowfield structure was reconstructed. Figure 5 presents typical impact pressure profiles at several Z locations in the corner flow.

Oil flow indications were used to locate points of separation and reattachment on the body surface. Because of the characteristics of separating flow, a converging oil flow line pattern was interpreted as a separation line and likewise, a diverging oil flow pattern was interpreted as a reattachment line. The oil flow used to locate these lines is shown in Fig. 6.

The salient features of this asymmetric corner flow, as indicated by the experimental data and summarized in Fig. 4, include one triple point at the intersection of the wedge and the plate bow shocks. This triple point is very similar to either one of the triple points shown in the Charwat and Redekopp[2] symmetric corner flow in that it generates a similar embedded shock and slip surface. The embedded shock of Fig. 4 provides an adverse pressure gradient which is felt far upstream in the boundary layer. The effect is first observed on a line approximately 45° from the x-axis or at $Z = 1$ where the boundary-layer cross flow first separates. This line has been termed S_1. An important feature of three-dimensional separation is the fact that, unlike two-dimensional separation, the dividing streamline is not the same streamline that reattaches. As a result of the open end feature of a three-dimensional separation bubble, flow entering the bubble is constantly scavenged away and must be replenished by a portion of the separation boundary layer. Hence, it is a higher energy streamline in this layer of scavenged flow that reattaches and not the low-energy separating streamline. It is this feature which primarily accounts for the high value of three-dimensional interference heating. The more energy that is available in the reattaching flow, the higher the heating rate will be. Within the bubble reverse flow occurs in the cross-flow plane much as it does in two-dimensional separation. As the cross flow continues, it gains enough energy from upper layers of flow to reattach, but almost immediately is forced to separate again because of the continuing adverse pressure gradient of the embedded shock. This reattachment and separation have been termed R_1 and S_2, respectively. The second separation bubble at S_2 appears to scavenge nearly all of the remaining plate boundary layer to such an extent that near R_2 no detectable viscous layer was present.

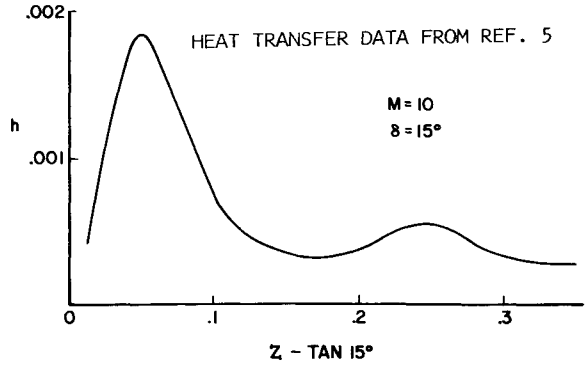

Fig. 7 Heat transfer on plate surface.

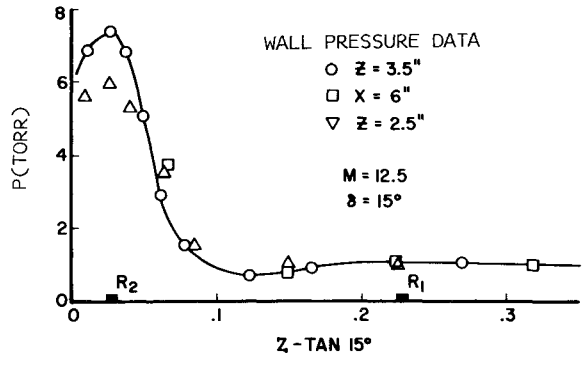

Fig. 8 Pressure readings on plate surface.

Other features of the flow include a small separation bubble (S_3) in the corner of the wedge with a reattaching streamline striking the plate near R_2. This small bubble was felt necessary to round off the corner and was not felt to be a dominant feature of the flow. Also present are two weak shocks generated by the thickening separation bubbles of S_1 and S_2. These shocks intersect the triple point embedded shock.

At the reattachment point, R_2, where the boundary layer is extremely thin, an inviscid finger extends down from the region of the triple point causing extremely high heating in this region. Figure 7 shows heating data taken from tests conducted by Schultz and Baker[5] using the same model tested in this study. Temperature-sensitive paint was used in these tests. The wall pressures shown in Fig. 8 also support the foregoing data in attesting to the high energy level present at R_2. Impact pressures of 270 mm were recorded within 0.1 in. of the surface at R_2 compared with 61 mm in the freestream. Stainback has shown similar heat transfer and pressure results for the corner flow problem.[6,7]

Using the data generated by this study, an attempt was made to reconstruct the corner flow in both the one and the two triple point configurations. This was deemed necessary to support the one triple point interpretation since the possibility existed of overlooking the second triple point if it were very weak or very close to the primary shock intersection. When the results of the calculated single triple point were applied to the data, impact pressures coincided within 10% in all regions around the point. A solution of similar accuracy could not be found, however, using two joined triple points in the corner flow. This result, combined with the fact that the wedge shock was capable of bending to match the single triple point solution, tends to confirm that only one triple point is present in the corner flow studied in the paper.

Conclusions

In this study, the flowfield of an asymmetric axial corner in laminar hypersonic flow has been measured. These measurements permitted the reconstruction of the induced inviscid flow structure. Only one point of interaction between the surface bow shocks was observed as opposed to two such triple points in the symmetric case. Also, a pair of separation bubbles were observed on the flat plate with two attendant separation shocks and two reattachment lines. Associated with the reattachment lines, surface heating and pressure measurements have shown two peaks of which the inboard value was significantly higher than that found at the outboard location. An inviscid supersonic jet, similar to the Edney type IV, was detected and found to impinge upon the plate surface near the second reattachment point. This jet resulted in high impact pressures and heating at this point.

References

[1] Gonar, A. L., "Exact Solution of the Problem of Supersonic Flow of Gas Past Some Three-Dimensional Bodies," *PMM (Journal of Applied Mathematics and Mechanics)*, Vol. 28, No. 5, 1964, pp. 974–976.

[2] Charwat, A. F. and Redekopp, L. B., "Supersonic Interference Flow Along the Corner of Intersecting Wedges," *AIAA Journal*, Vol. 5, No. 3, March 1967, pp. 480–488.

[3] West, J. E. and Korkegi, R. H., "Interaction in the Corner of Intersecting Wedges at a Mach Number of 3 and High Reynolds Numbers," ARL 71-0241, Oct. 1971, Aerospace Research Lab., Wright-Patterson Air Force Base, Ohio.

[4] Kutler, P., "Supersonic Flow in the Corner Formed by Two Intersecting Wedges," *AIAA Journal*, Vol. 12, No. 5, May 1974, pp. 577–578.

[5] Schultz, H. D. and Baker, R. C., "Pressure and Heat Transfer Measurements in Regions of Three-Dimensional Shockwave-Boundary Layer Interactions," LMSC-D157341, March 1972, Lockheed Missiles and Space Co., Sunnyvale, Calif.

[6] Stainback, P. C., "Heat Transfer Measurements at a Mach Number of 8 in the Vicinity of a 90° Interior Corner Aligned with the Free-Stream Velocity," TND-2417, 1964, NASA.

[7] Stainback, P. C., "An Experimental Investigation at a Mach Number of 4.95 of Flow in the Vicinity of a 90° Interior Corner Aligned with the Free-Stream Velocity," TND-184, 1960, NASA.